Coastal Landforms of the Basque Coast UNESCO Global Geopark – From Inventory to Geomorphological Map

Report for the Year 2024

Paola Coratza, Piotr Migoń, Mauro Soldati, Vittoria Vandelli

Coastal Landforms of the Basque Coast UNESCO Global Geopark – From Inventory to Geomorphological Map

Report for the Year 2024

Paola Coratza[1], Piotr Migoń[2], Mauro Soldati[1], Vittoria Vandelli[1]

[1] Department of Chemical and Geological Sciences, University of Modena and Reggio Emilia, Italy
[2] Institute of Geography and Regional Development, University of Wroclaw, Poland

1. Introduction

1.1. Project context

The Basque Coast UNESCO Global Geopark (UGGp) is renowned for its outstanding geological heritage, primarily the record of deep marine sedimentation in the Cretaceous and Paleogene, which produced thick flysch series, magnificently exposed along the coast. The global significance of the flysch is confirmed by the establishment of two Global Boundary Stratotype Sections and Points (GSSPs), marking the base of the Selandian and Thanetian stages of the Paleogene (IUGS, 2022). In addition, the coastal exposures within the Geopark, stretching along approximately 15 km, represent a scenery of superb aesthetic values, with textbook examples of wave-cut platforms, cliffs, and structure-controlled inlets (Aranburu et al., 2015; Cearreta et al., 2021; Morales et al., 2021; Hilario et al., 2023). However, scientific understanding of the geomorphology of the coast within the Geopark boundaries appears limited, with even landform inventories being apparently incomplete. More specifically, the occurrence of coastal landslides has been noted, and some have been observed in the past few decades, but not investigated in detail.

This project, presented to the Board of the Basque Coast UGGp and approved to be implemented, aims to fill this gap and provide more systematic knowledge about the diversity of coastal landforms, with the particular focus on coastal landslides. It is intended for two years. This report arises from Phase 1, which involved a preparatory work, field work in July 2024 and subsequent desktop research.

1.2. Scope and methods

The preparatory work involved examination of available materials such as scientific papers published so far, inventories of geosites within the Geopark, geological and topographic maps, popular science materials prepared by the Geopark, and Google Earth imagery. This helped to define localities of potentially highest relevance and plan the schedule of field work campaign. During the field campaign we visited most sections of the coast between Ondarroa to Zumaia, and walked extensively along the beach-rock platform/cliff transition between Zumaia and Sakoneta, suggested to us as the most relevant part of the coast. We also got a wider perspective from a boat trip along the coast. Qualitative landform recognition was supplemented by simple measurements using laser rangefinder. Both ground photographs and drone imageries were collected. The latter were acquired using a drone DJI mini 2 SE flying at different elevations from the ground, spanning from few metres to 60 metres, and recording pictures from variable angles. Additionally, remote sensing data, including orthophotographs from 1945 to 2022 and multitemporal LiDAR-derived Digital Terrain Models (DTMs) with a spatial resolution of 1 m from 2008 to 2017, were acquired to provide further evidence of the temporal evolution of the investigated coastal stretch. The LiDAR data were downloaded from the Spatial Data Infrastructure of the Basque Country geoportal (http://www.geo.euskadi.eus). Moreover, a comparison of the Digital Terrain Models (DTMs) from 2017 and

2008 was conducted using DEM of Difference technique for calculating the differences in elevation. These methods included subtractive analysis, where the elevation values of 2008 were subtracted from those of 2017. Google Earth images spanning from 1991 to present were also used. Additionally, ground motion data from the European Ground Motion Service (EGMS) were utilized, providing access to information on ground motion across Europe based on satellite radar interferometry, specifically using synthetic aperture radar (SAR) data from Sentinel-1 satellites.

2. Geological and geomorphological setting

2.1. Geology

The coastal stretch within the boundaries of the Basque Coast UGGp lies between the mouth (estuary) of the Urola River in Zumaia the east and the mouth of the Artibai River in Ondarroa. Based on lithology and rock age, it can be divided into two sections of comparable length. The western section between Ondarroa and the headland of Mendatagaina is eroded in Lower Cretaceous (Albian) flysch formations, mainly developed as grey shales, with intercalations of sandstones (greywackes) and, locally, the presence of conglomerates and breccia. Collectively, they are known as "black flysch". The eastern section is eroded in younger flysch formations, spanning the interval from the Cenomanian (Upper Cretaceous) to the beginning of the Eocene. Here the dominant lithologies are marls, shales, limestones, and subordinately sandstones, and the flysch is calcareous, which gives it a yellowish colour. The boundary between the two sections is of tectonic origin, taking the form of a N–S-trending Andutz Fault, which runs along the western side of Mendatagaina promontory and continues inland. In addition, these two sections differ in terms of the structural grain and the dominant strike of the strata. In the western section the general strike is W–E, hence broadly parallel to the coastline. In the eastern section it is more varied, from NNW–SSE close to the Andutz Fault to WNW–ESE in Zumaia. Thus, the flysch strata are intersected by the shoreline at different angles in different places along the coast, with implications on the appearance of coastal landforms.

2.2. Geomorphology

The overall geomorphology of the Basque Coast UGGp is steep and mountainous, with the highest peaks exceeding 600 m a.s.l. The rugged, karstic inland terrain, dissected by numerous V-shaped valleys, is sloping towards the coastline in the north. Altitudes along the coast, within a 2-km-wide belt, locally reach 300 m a.s.l., but are typically up to 200 m a.s.l. The cliffs themselves (here understood as bare rock slopes facing the sea) vary in height, locally exceeding 100 m, and are in many places followed upslope by soil-covered, but still extremely steep, impassable slope sections. Rock exposures appear more common and extensive in the eastern section of the coast, where the calcareous flysch occurs.

Local water-divide ridges close the coastline are typically rounded and may retain approximately constant elevation over hundreds of metres. These are present, for instance, to the west of Zumaia, towards Elorriaga, and to the west of Mutriku. Further examples occur more inland, at higher elevations (e.g., a nearly level water divide from Ganeta (443 m) to Endoia (429 m), to the west of the town of Zestoa). Whether these flattened ridges represent remnants of former low-relief landscapes ("planation surfaces", specifically marine abrasion surfaces) and can be used to reconstruct long-term landform evolution in the coastal zone, it cannot be determined at present. However, there were attempts to use the karstic landforms, especially the conical shapes of limestone hills, to reconstruct the geomorphic evolution in the past 5 million years or so (Aranburu et al., 2015).

The coastline in the Geopark is relatively straight, with only a few more distinct rocky promontories (Eskilantxarri next to Saturraran Beach near Ondarroa, Alkoleako to the east of Mutriku, Mendatagaina,

Talaimendi in Zumaia), and none longer than 1 km. The continuity of the rocky coastline is interrupted by four estuaries, in Ondarroa, Mutriku, Deba and Zumaia. The latter is also the widest, more than 300 m at the mouth. Minor streams are not graded to the current mean sea level and are hanging above the cliff faces.

3. Diversity of coastal landforms – an overview

The coastline in the Basque Country UGGp is primarily erosional and subject to retreat in the long term. Hence, the majority of landforms along the coast is erosional, with hard rock cliffs and abrasion (wave-cut) platforms being dominant. However, depositional landforms occur too, especially within more sheltered settings such as minor bays and estuaries. This section of the report intends to provide a preliminary inventory of coastal (and marine) landforms within the Geopark, with brief description and supporting photos

3.1. Erosional landforms

3.1.1. Cliffs

Cliffs dominate the coastal scenery of the Basque Coast UGGp. Their aggregate length is approximately 14 km, which is 50% of the total effective coastline length. They reach variable height, from less than 10 m to more than 100 m (Fig. 1). Their extension (length) is also variable, from localized presence at promontories to continuous sections several kilometres long. Most cliffs expose flysch rocks in situ, but locally low cliffs in colluvial deposits exist.

Fig. 1. Variable cliff height between Zumaia and Sakoneta, as observed from the sea.

The detailed morphology of cliffs cut in flysch rocks varies, depending on the angle between the strike of the flysch strata and the coastline, as well as reflecting variability in the dip of flysch units. For example, at Playa de Itzurun the cliff line is straight and almost perfectly accordant with the strike of the flysch strata of Danian age, whereas the cliff face itself is composed of exposed bedding planes (Fig. 2). An analogous situation from the area of "black flysch" occurrence is illustrated by Fig. 3. In contrast, at Bay of Sakoneta the cliff line intersects the strike of the flysch strata almost at the right angle, with beds of various resistance exposed in the cliff face (Fig. 4).

Fig. 2. Cliff morphology accordant with the strike and dip of flysch strata (Playa de Itzurun, Zumaia).

Fig. 3. Cliff morphology generally accordant with the strike and dip of black flysch strata (Arranomendi) – a view from Mendatagaina viewing point.

Given the considerable extent of coastal landslides in the Basque Coast UGGp, especially in the eastern part built of the calcareous flysch, it is useful to make a fundamental division of the cliffed coastline into:

- wave-undercut cliffs, whose morphology is entirely dependent on the continuous interplay between marine forces and local geological structure, with bedrock in situ exposed in the cliff face, up to the upper rim. In these cases, bedrock outcrops are subject to direct wave attack (Fig. 5). Cliff morphology in detail, in turn, reflects the strike of flysch strata in relation to the orientation of the coastline. If the strike is perpendicular, cliffs are composed of alternating ribs and recesses in more and less resistant layers, respectively (Fig. 5). If the strike is parallel, the cliff face may coincide with

an exposed bedding plane (or a few closely spaced planes). It is then remarkably smooth over tens of metres (Fig. 6)

- landslide-modified cliffs, whose morphology reflects the occurrence of a coastal landslide and its subsequent modification by younger displacements. In these cases, waves attack colluvial packages and deformed flysch strata, resulting in lower cliffs of considerably less height (<10 m). However, much higher rock slope sections may occur further upslope, up to the landslide crown (Fig. 7).

The wave-undercut cliffs are associated with a range of minor landforms and these will be presented below, whereas three specific examples of coastal sections which show effects of large-scale landslide remodelling will be presented in section 4.

Fig. 4. Cliffs discordant to the strike of the flysch strata (Bay of Sakoneta).

Fig. 5. Wave-undercut cliff at Talaimendi, with no evidence of landslides (Zumaia). Individual beds, standing vertically, are perpendicular to the cliff base.

Fig. 6. Example of a cliff, where the strike of the strata is roughly parallel to the cliff base, resulting in smooth appearance of the rock face (Mendatagaina promontory).

Fig. 7. Cliff section of the coastline, heavily reshaped by landslide processes (between Zumaia and Sakoneta). Note the low cliff in the lower right due to wave undercutting of landslide colluvium.

- **notches**. They are not very common along the Basque Coast UGGp coastline and those identified are not particularly distinctive. Reasons may reside in the properties of flysch strata exposed at the base of the cliffs. Notches are typically associated with more massive lithologies, with fewer discontinuities, or exploit horizontal lines of structural/lithological weakness. In addition, the rock above the notch should be strong enough to withstand tensile stress and not to collapse into the void created by wave undercutting. None of these conditions seems to be fulfilled at the coastline of the Basque Coast UGGp. However, in a few places rounded basal recesses have been found and these may be tentatively interpreted as coastal notches (Fig. 8).

Fig. 8. A notch in the coastal section beneath Elorriaga. The ruler is 1 m high.

- **<u>marine (abrasion) caves</u>**. These occur in various places along the coast, including Playa de Itzurun in Zumaia and Mendatagaina promontory as the best examples. In addition, there occur minor caverns/hollows at the base of the cliffs. Marine caves are evident rock-controlled features and develop through preferential erosion of weaker strata after an outcrop of a more resistant bed is breached by wave attack and waves get direct access to the weaker lithology behind (Fig. 9). Marine caves may also form due to preferential erosion of a line of structural weakness (fault, fracture zone) perpendicular or oblique to the general orientation of the cliff. Some marine caves at Playa de Itzurun seem to owe their existence to the combination of both factors (lithology and structure) (Fig. 10).

Fig. 9. One of marine caves at Playa de Itzurun, exploiting a group of less resistant layers.

Fig. 10. Some marine caves at Playa de Itzurun owe their origin to the combination of weak resistance of rock and the presence of prominent fractures perpendicular to the cliff line. One in the middle has already been enlarged to a cave, whereas one to the left illustrates an initial stage.

- **cliff-base talus**. Many cliff faces extend down to the waterline and are subject to direct undercutting. However, some are separated from the sea by accumulations of boulders, which also provide temporary protection against wave attach by armouring the cliff base (Fig. 11). Thus, these sections of the cliff line become more stable (still being subject to weathering and other processes) until the boulder armour is destroyed by waves. Cliff-base talus is derived from mass movements within the cliffs themselves, which may have been free falls from an undercut cliff or slides along exposed, steeply dipping bedding planes. Both are presented in the Basque Coast UGGp. The volume of the cliff-base talus varies, which reflects both the magnitude of the fall/slide, as well as the age of the talus. Over time, with continuing wave attack and boulder weathering, the dimensions of boulders will decrease and their density will diminish. A particularly voluminous talus is present beneath the promontory of Talaimendi in Zumaia (Fig. 12).
- **promontories**. The general course of the coastline in the Basque Coast UGGp is straight (notwithstanding interruptions by estuaries), but in a few places distinct bedrock promontories exits. The largest of them is Mendatagaina, approximately 250 m long and 230 wide at the head (Fig. 13). Other promontories include Algorri in Zumaia, Alkoleako next to Mutriki, and Eskilantxarri at the Saturraran Beach next to Ondarroa. Promontories build of bedrock typically indicate the presence of more resistant rocks, so that more efficient erosion on either side of the resistant outcrop progressively isolates a headland jutting into the sea. Thus, the Mendatagaina promontory owes its existence to the N–S outcrop of resistant limstones of the Itziar Formation, perpendicular to the general orientation of the coastline. The Algorri promontory is built of a relatively narrow belt of Danian flysch (Atzgorri Formation), but dominated by resistant limestones. Greywackes build the promontories of Alkoleako and Eskilantxarri, whereas less resistant shales occur next to them. In all these cases the dip of the strata is sub-vertical or very steep, above 40°.

Fig. 11. Talus composed of thin rock slabs below the cliff, derived from a planar slide.

Fig. 12. Big boulders build the talus beneath the Talaimendi promontory (view from the cliff upper rim). The flysch exposed in the slope above does not include beds which could supply boulders to the talus and their source is likely elsewhere.

Fig. 13. Promontory of Mendatagaina from the west. Note the rock-fall scar on the right, along with boulder talus below, as well as entrances to two marine caves on the left.

- **stacks** (one site, near Ondarroa). Stacks are rock landforms separated from the main cliff line and standing in isolation within an abrasion platform. Their base may be periodically exposed or permanently submerged. The only locality in the Basque Coast UGGp where geomorphic features similar to stacks occur is Eskilantxarri next to Ondarroa. Here the continuity of the promontory (see above) is almost completely broken and a distinctive bedrock crag, approximately 10 m in height, rises from the rock-cut platform (Fig. 14).

Fig. 14. Composite stack of Eskilantxarri, next to the Saturraran beach in Ondarroa.

- **hanging valleys**. In several places along the coast hanging valleys are present. These are understood as inland valleys whose floors are not graded to the level of the wave-cut platform but truncated by the cliffs. The height difference between the suspended valley floor and the cliff base varies from 2–3 m to around 10 m (Fig. 15). In addition, topography suggests that some V-shaped erosional valleys, once likely connected with the sea, have been truncated by landslides, and their floors are now

suspended above the landslide crown (Fig. 16). The area around Elorriaga provides instructive examples. Hanging valleys in general indicate inability of fluvial incision to respond to the change (decrease) of distance to the base level. Some hanging valleys are dry or host only episodic flow.

Fig. 15. Hanging valley in Sakoneta. Dashed line shows the suspended valley floor, an arrowed line indicates the height of suspension.

Fig. 16. The mouth of a V-shaped valley in Elorriaga is hanging high above the cliff, which has been considerably remodelled by landslides and subject to episodic retreat.

Of particular interest is the hanging valley morphology immediately to the west of Zumaia (Fig. 17). A V-shaped valley begins at Saskarategana and continues in NE direction for approximately 1200 m, until the valley floor is truncated by the cliff some 10 m in height (Fig. 18). Another dry valley begins at Algorri and

continues for 900 m to the east, partly within the limits of the built-up area of Zumaia, until it reaches the former town harbour basin (now the Amaia plaza). This valley, in turn, is truncated at its head and appears to miss the upper reach (Fig. 19). It is very likely that they once former one valley tract, whose continuity was interrupted by marine abrasion and cliff retreat. The lack of flow in the lower reach confronted with the very well-developed valley shape gives support to this hypothesis. However, more research would be needed to confirm or reject this hypothesis.

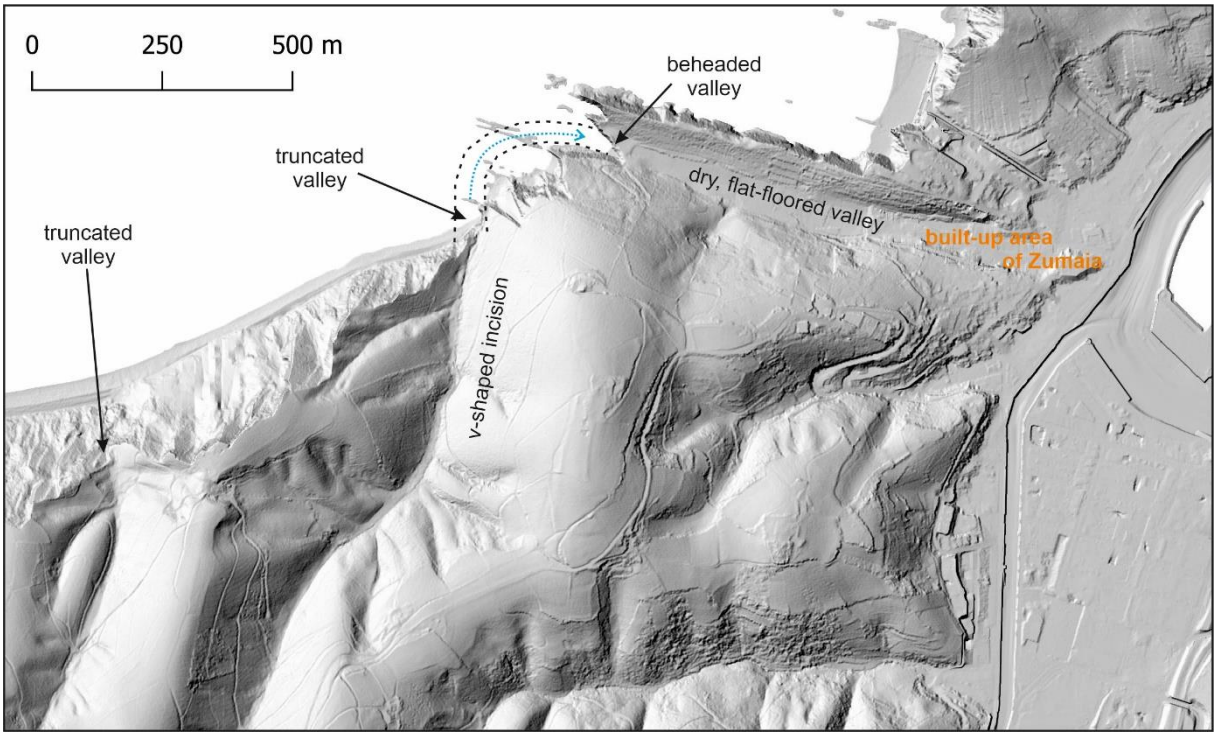

Fig. 17. Probable truncation and beheading of a valley next to Zumaia due to cliff retreat. Further to the west another v-shaped valley is truncated by a cliff, here due to retrogressive landsliding.

Fig. 18. Truncated upper part of the valley shown in Fig. 17.

Fig. 19. Beheaded lower part of the valley, now dry, shown in Fig. 17. The valley floor is sloping from right to left.

3.1.2. Wave-cut platforms

Wave-cut (abrasion) platforms belong to the landmarks of the Basque Coast UGGp. The most renowned locality is Sakoneta, but in fact the platforms coexist with cliffs along most of the coastline. They are almost continuous between Zumaia (Algorri) and Sakoneta, at the foot of Arranomendi, and to the west of Mutriku. They are developed in both the calcareous flysch and "black flysch" (Fig. 20, 21), but those in the "black flysch" have less ordered microrelief. These differences are attributed to the geological composition of the flysch itself.

The calcareous flysch consists of repetitive alternations of thin strata of limestone, sandstone and marl, hardly more than 1 m thick. Each layer has its own strength and resistance to weathering and abrasion, reflected in its appearance within the platform. More resistant layers stand out, forming sharp ridges: "teeth" (narrow) or "ribs" (wider), whereas less resistant layers are marked by linear troughs. The height of upstanding elements varies, depending on the thickness of strata and relative differences in strength, from only a few tens of centimetres up to 3–4 m. The dip of strata is another factor controlling the microrelief of the platforms. If the dip is not far from horizontal (up to 20° or so), the ridges resemble cuestas, with smooth, gently sloping ramps on one side, and steep faces on the opposite one. With an increasing dip the ridges become more and more steep and symmetrical, whereas at very steep dip almost vertical fins form (Fig. 22). At the most local scale, facetted microrelief of the ridges reflects orthogonal jointing of the flysch, with individual facets following joint surfaces.

The "black flysch" is more chaotic and lacks regular repetition of strata of contrasting resistance to abrasion. Moreover, even where such alternations exist, the strike is generally parallel to the coastline, unlike the calcareous flysch, where it is at an angle or close to perpendicular. Therefore, platforms lack regular microrelief and tend to be sloping ramps with wavy morphology, as at Mutriku. This smoother, ramp-like relief allowed for the development of minor erosional landforms within the platforms, which are almost absent in the calcareous flysch – the potholes (see below).

Fig. 20. Wave-cut platform in thinly-bedded calcareous flysch next to Elorriaga.

Fig. 21. Ramp-like, undulated surface of a ramp-like wave-cut platform in “black flysch” next to Mutriku.

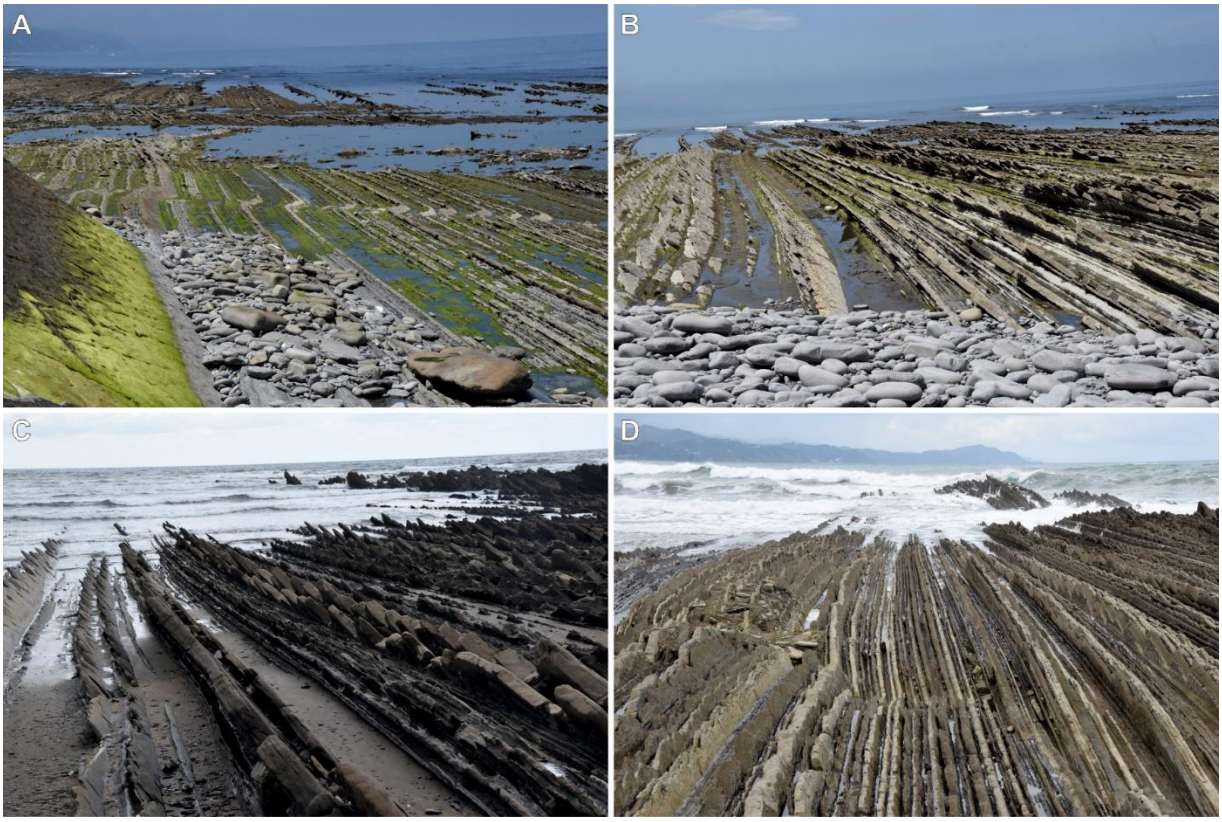

Fig. 22. Details of microrelief of wave-cut platforms in the calcareous flysch, depending on the dip of the strata. Panel A shows the least dip, increasing to moderate in panels B and C, whereas in panel D the dip is close to vertical.

Various minor landforms are associated with the wave-cut platforms:

- **joint-aligned clefts**. In platforms developed in the calcareous flysch, especially at Sakoneta, linear, cross-crossing clefts occur (Fig. 23). They follow major joints which strike in different directions. As the discontinuities are the natural lines of weakness, abrasion forces exploit them more effectively than the intervening, more massive compartments. These clefts are up to a few tens of centimetres wide and may be as deep as 1 m, with most part being submerged. During low tide, these parts turn into strings of pools.
- **potholes**. Circular and oval hollows incised into subhorizontal surfaces are best developed in the "black flysch". They are abundant within the platform to the west of Mutriku. Their dimensions vary from 10 – 15 cm in diameter and less than 10 cm in depth, to much larger features, approximately 1 m across and up to 50 cm deep (Fig. 24). They typically have gravel and pebbles inside, which are abrasive tools set in motion by waves during high tide. Some potholes, especially the oval ones, have developed along fracture lines and show structural control. Locally they occur in strings, one after another (Fig. 25). Other potholes seem to be initiated by preferential erosion of siliceous concretions inside the flysch. These concretions, being more resistant, are upstanding elements and protect the flysch below, causing minor undulations of the platform. However, they are also easy to detach from their base by strong waves and if this happens, a hollow emerges on top of such an undulation (Fig. 26). These can then develop into potholes.
- **boulders**. In various places one can observe isolated boulders on the platform, which cannot be connected with any obvious source such as rockfall from the cliff nearby. Striking examples occur between Elorriaga and Sakoneta, where the boulders are up to 3 m long and 1 m high, although thin slabs are also present (Fig. 27). Lithologically they also represent the flysch. As long as they exist, they act as protective caps to the abrasion platform below.

Fig. 23. Joint-aligned clefts (indicated by arrows) within the wave-cut platform at Sakoneta.

Fig. 24. Large circular pothole in “black flysch” in Mutriku, filled with pebbles.

Fig. 25. Strings of small elongated potholes in “black flysch” in Mutriku.

Fig. 26. Evolution from a protruding siliceous concretion (A) to the small pothole (C). (B) shows an intermediate stage, where the concretion is partly broken along a crack, one part has been removed and a small basin originated in this place. Wave removal of the remaining part of the concretion will produce a hollow similar to that of (C).

Fig. 27. Large boulders on the wave-cut platform, between Elorriaga and Sakoneta.

3.2. Depositional landforms

Depositional coasts are in the minority in the Basque Coast UGGp, mostly inside the estuaries (Fig. 28). In addition, many open coast beaches are in fact associated with the cliffs, forming narrow belts of predominant coarse gravel and small boulders between the cliff base and the wave-cut platform. This is the case of a long gravel beach between Algorri and Elorriaga. Pocket gravel beaches between two rocky promontories occur in several places, such as Eskilantxarri, Alkoleako, and Itzurun (Fig. 29).

Considering the size of beach material, two types may be distinguished:

- **Sandy beaches**. These occur mainly in estuaries (Ondarroa – Saturraran Beach – Fig. 30, Deba, Zumaia, at the mouth of the River Urola), whereas the sandy beach at Itzurun in Zumaia is not associated with a river mouth. Two beaches in Zumaia are 250 m long, whereas the one in Deba is more than 1 km long (including the break – the mouth of River Deba). The width varies depending on the tide and may attain approximately 300 m at low tide (Deba).
- **Gravel/boulder beaches**. Small gravel beaches are present in sheltered bays (pocket beaches), whereas two longer stretches of gravel/pebble beach occur between Algorri and Elorriaga (1.4 km) and to the west of Mendatagaina promontory (0.7 km) (Fig. 31). In each case they are associated with large, laterally extensive landslides behind, which probably supplied considerable amount of material to be then reworked and redeposited by waves. Individual rock fragments are typically very well rounded (Fig. 32).

Fig. 28. Deba estuary, where depositional areas have been almost entirely taken by urbanization, except the beach.

Fig. 29. Gravel-boulder pocket beach next to Alkoleako promontory.

Fig. 30. Sandy beach of Saturraran.

Fig. 31. Long stretch of boulder-gravel beach along the landslide-remodelled cliffs between Elorriaga and Algorri.

Fig. 32. Close view of rounded boulders forming the beach.

Along the gravel/boulder beach between Algorri and Elorriaga one can observe several levels of berms (beach-ridges), accounting for the step-like morphology of the beach (Fig. 33). Here the distance from the wave-cut platform/beach boundary to the base of scree cones below the cliffs is 37 m, with the elevation difference of three consecutive ridges of 0.6 m, 0.7 m and 1.6, going inland. Normally this type of relief is attributed to the annual cycle of tides, with the crest of the highest ridge marking the uppermost limit of a spring high tide, and the lower ridges indicating falling high tide levels. However, very high and distinct berms, beyond the extent of tides, indicate exceptional storm events. No detailed investigation of berms at this section of the coast was conducted and it is not possible to provide unequivocal explanation of these features.

Fig. 33. Step-like profile of a berm. Considerable volume of driftwood behind the berm (to the left) is consistent with the storm origin of this feature.

Mudflats, which likely existed inside the estuaries along the Basque Coast UGGp coastline, have almost completely disappeared due to centuries of anthropogenic reshaping. The areas of their former occurrence were taken over by built-up areas, transportation corridors, and harbours. A small remnant is present in Zumaia, next to the marina, inside the mouth of the River Urola (Fig. 34). Next to this locality and further seaward, a small **dune field** survived, even though partly vegetated and built-up. It is located immediately inland from one of the sandy beaches (Fig. 35).

Fig. 34. Succession of depositional surfaces, from beach (A) through the dune field (B) to mudflat (C), in the mouth of River Urola in Zumaia.

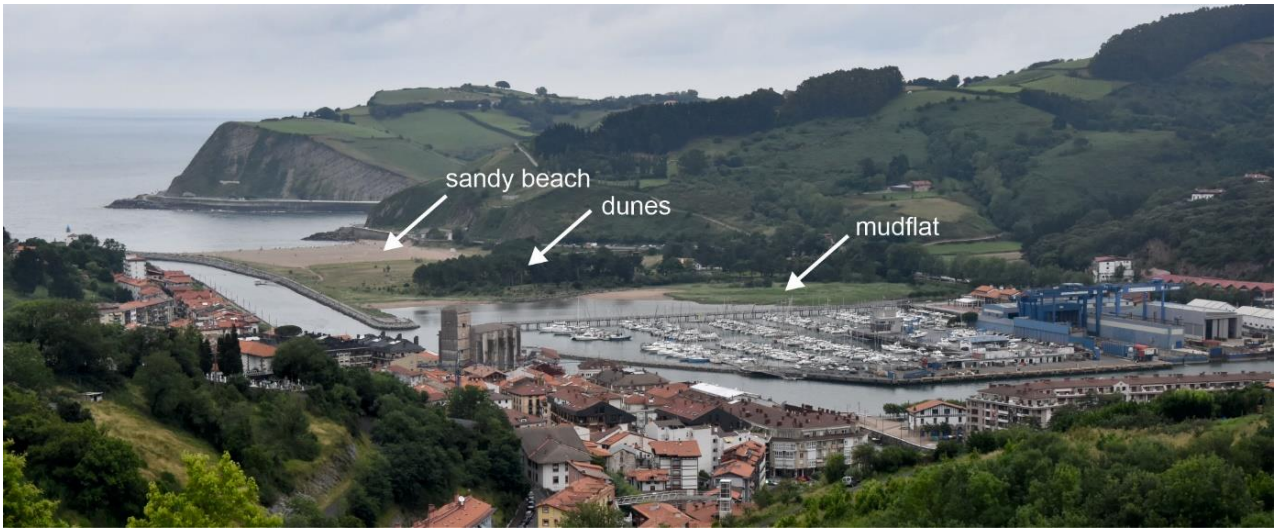

Fig. 35. The same succession of depositional surface – ground photo from a hill above Zumaia.

4. Coastal landslides

4.1. Diversity and structural controls

The intersection of flysch strata with the shoreline at different angles in different places along the coast (see section 2.1) is of fundamental importance for the initiation, mechanisms, and evolution of coastal landslides. The latter are strictly controlled by the dipping of the strata. When the dip of the strata is parallel to the coastline, rock sliding phenomena prevail – with failure surfaces along the bedding planes, whereas when the dip of the strata is (sub)perpendicular to the coastline, landslide mechanisms tend to be more complex, also in relation to the mechanical behaviour, thickness and related resistance to erosion of individual strata.

Within a few landslide bodies, flysch deformation and folding has occurred, resulting in peculiar landforms. In this respect it should be noted that landslides in flysch terrains can cause significant deformation, as the layered sedimentary structure of flysch comprising lithotypes with different mechanical behaviour is prone to flexing under the stresses associated with movement.

Deformation processes in flysch terrains are influenced by both the rock intrinsic properties and external forces. The mechanisms that lead to folding can be related to a combination of acting forces, mechanical properties of the rocks, and exacerbating external conditions, as outlined below (cf. Cruden and Varnes, 1996):

- Compression and shearing. Gravity-induced processes apply uneven compressive and shearing forces on flysch layers, causing their bending and buckling, which can evolve into open or closed folds. As a result of their displacement, the flysch layers undergo additional tension, which can amplify the folding.
- Creep and progressive folding. Especially in cases of creep (slow, but persistent movement), flysch beds can develop gradual, wave-like folds. Over time, and with continued movement, the folds become sharper as the rock mass adapts to the consistent stress from movement.
- Folding susceptibility. Flysch often consists of alternating weak clay-rich layers and harder, sandstone layers, the former being much more easily deformed than the latter. This layering enables differential movement, where weaker layers can slip or fold under pressure while more resistant layers stay more intact.
- Factors enhancing deformation. Factors such as rainfall, seismic activity, and freeze-thaw cycles exacerbate folding. For instance, episodic rainfall contributes to water infiltration, increasing pore pressure within clay layers, which further lubricates and destabilizes the strata, promoting folding.

The interaction of gravity-induced forces with the stratification of the flysch thus creates complex deformations, often resulting in folding that is visible as undulating or warped layers on exposed rock faces. Such processes occur along the Basque Coast UGGp coastline, producing remarkable flysch deformations at the Pikote and Baratzazarrak landslides (cf. Sections 4.2, 4.3).

4.2. Pikote landslide

The Pikote landslide is located along the coastal stretch between Elorriaga and Zumaia, in the locality of Andikaraerreka. Its length along the coastline is some 360 m, while the width varies from approximately 200 m in the central part to 150 m at its flanks (Fig. 36). The edge of the landslide scarp has an approximate length of 400 m and the landslide deposit covers some 45,000 m^2.

The description below is based on varied sources of information: (a) field observations carried out along the landslide body and at its toe; (b) photographs, also taken with the drone, acquired during field surveys carried out in July 2024; (c) high-resolution DTM of the area; (d) multitemporal orthophoto images

from 1945 to 2022; and (e) European Ground Motion Service (EGMS) dataset providing information on surface movements.

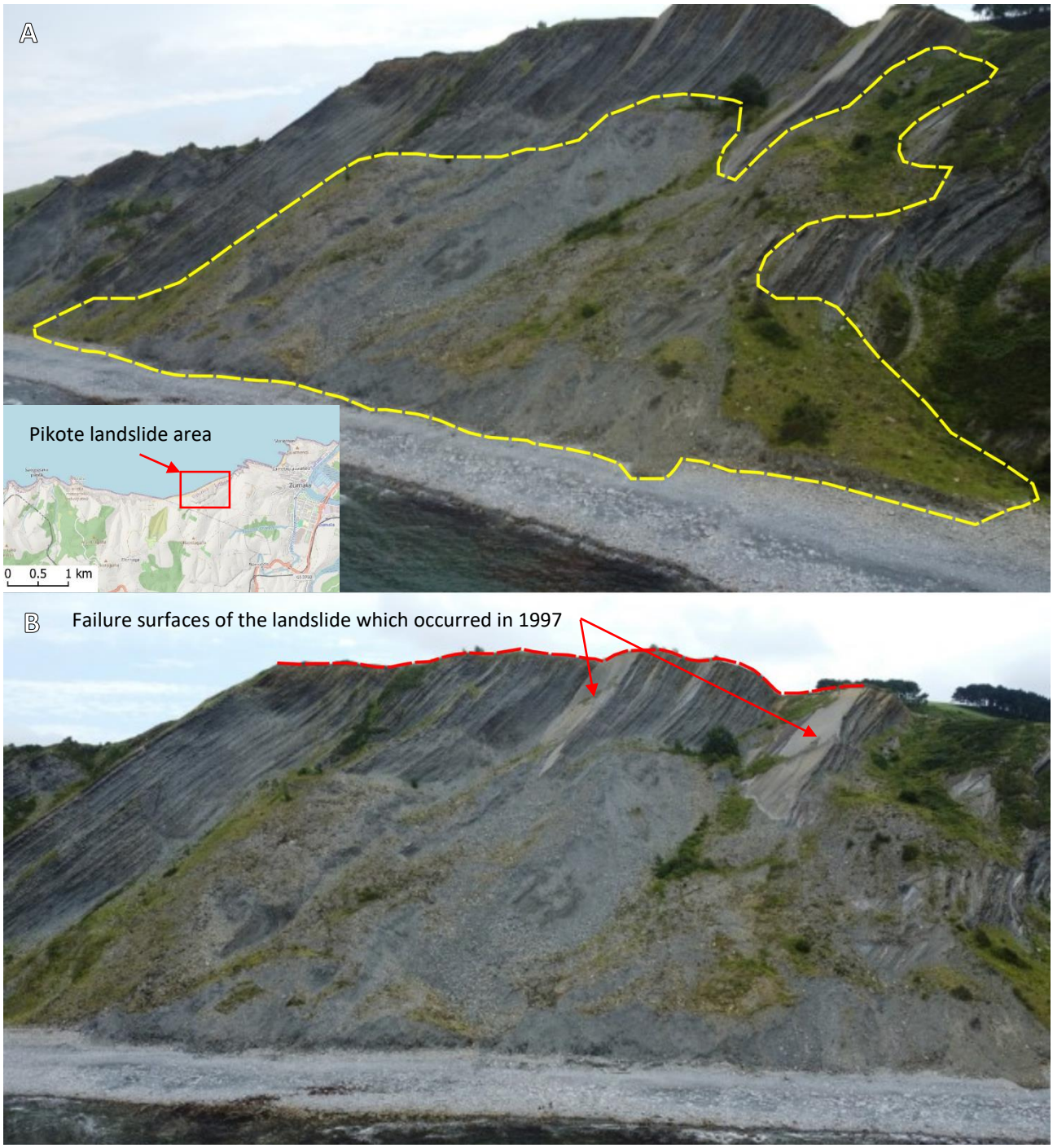

Fig. 36. View of the Pikote landslide taken from the drone on 14th July 2024: (A) the yellow dashed line delimits the landslide body (depositional area); (B) the red dashed line indicates the approximate outline of the landslide scarp edge.

The absence of vegetation along the slope, visible on a sequence of historical orthophotos dating back to 1945, suggests that the area has been unstable at least since that time. One major landslide event occurred in 1997, as documented in historical records, and resulted in the loss of livestock and agricultural land. This is corroborated by comparing aerial photographs from 1991 and 2001. In the 2001 image, there is clear evidence of slope retreat compared to 1991, along with a substantial accumulation of landslide debris at the base of the slope, near the shoreline (Fig. 37).

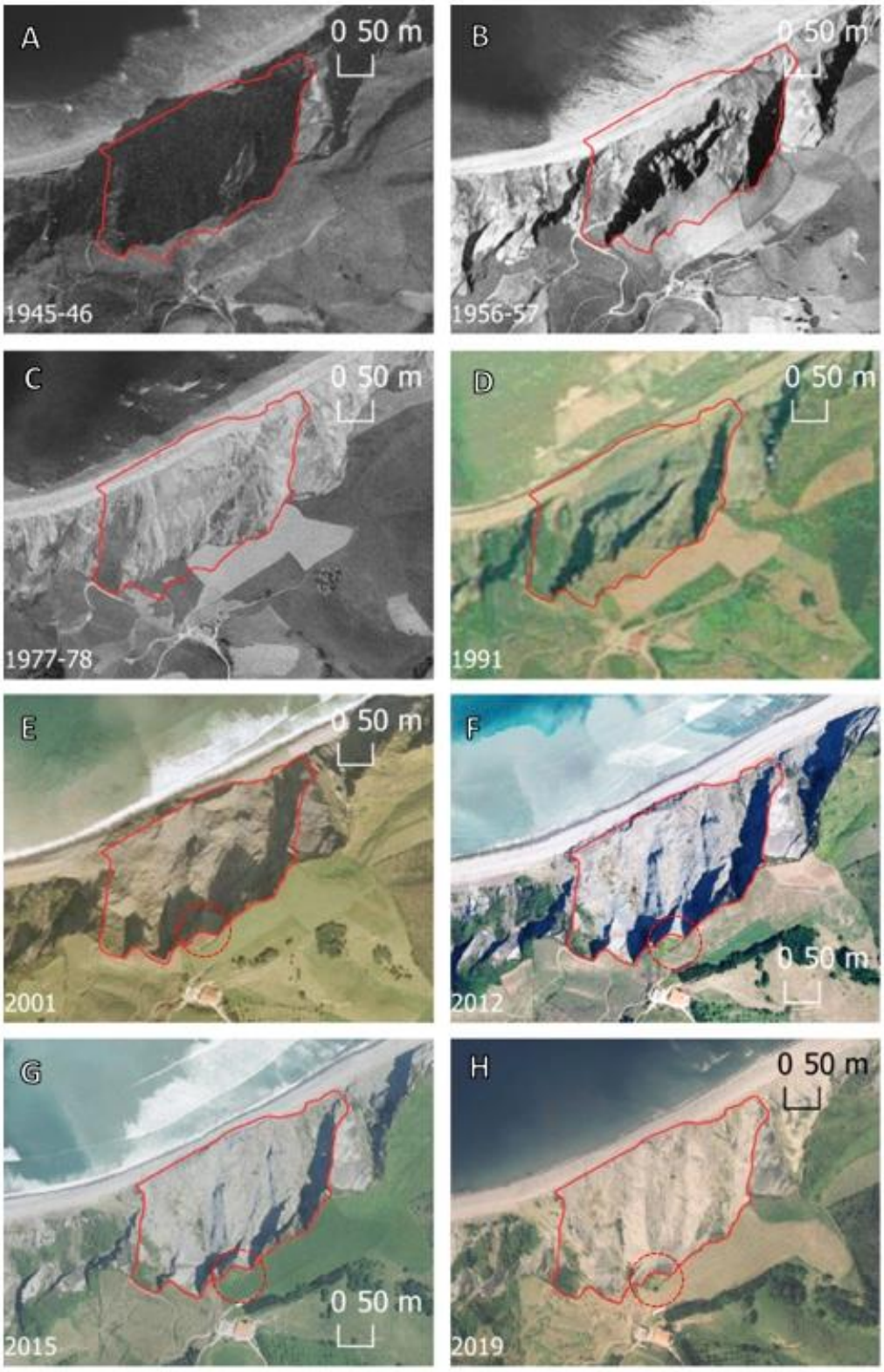

Fig. 37. Orthophoto images of Pikote landslide from 1945 to 2019. Red line indicates the approximate extent of the landslide area as seen in the 2019 orthophoto. In (A), (B), and (C), the shoreline is straight, and the slopes within the landslide area appear almost completely devoid of vegetation, which suggests recurrent instability. In (D), a debris cone has encroached onto the beach, extending the shoreline seaward. In (E), (F), (G), and (H), the debris deposited on the beach appears to be progressively eroded by sea action. The red circle highlights the presence of a block along the landslide scarp in the shape of a prism, partially detached from the main scarp.

The difference in elevation between the DTMs of 2017 and 2008 (Fig. 38) reveals a significant displacement in the central part of the landslide deposit, with a lowering of several meters, particularly localized in the core area of the deposit. This indicates ongoing downslope movement of landslide body, which however has not resulted in the seaward shift of the shoreline, apparently due to efficient removal of incoming landslide debris by storms and waves. In contrast, some sectors of the landslide deposit show an elevation increase, likely due to the deposition of new material. The spatial resolution of the DTM is 1 m × 1 m, which can be considered as the indicative accuracy of this analysis. It should be noticed that the DTM may have some artefacts which may alter the results of the DoD analysis. However, the results achieved suggest that the landslide deposit is undergoing significant instability, further investigations being required to more accurately quantify the mode and rate of displacement.

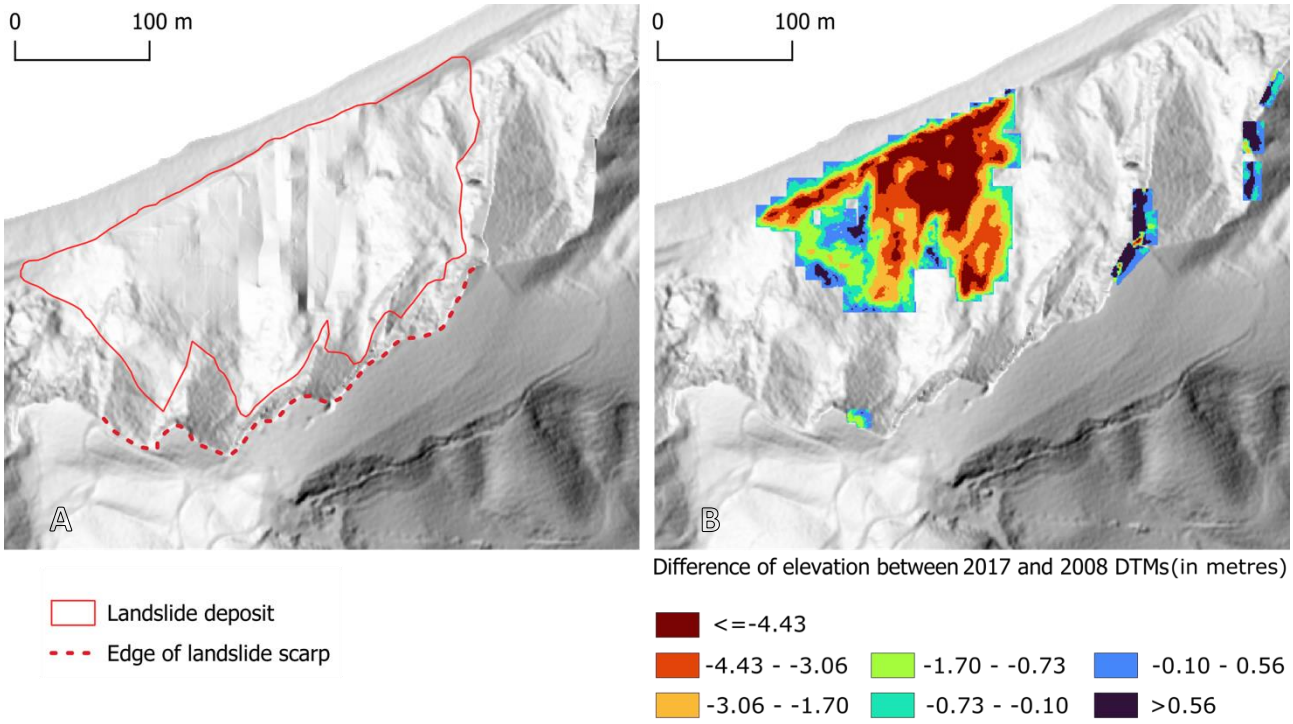

Fig. 38. (A) Pikote landslide on shaded relief obtained from a high-resolution DTM of 2017. (B) DEM of Difference (DoD) for the years 2017–2008. Areas where no changes occurred are left non-coloured.

Fig. 39 shows the EGMS (European Ground Motion Service) Ortho dataset used for the Pikote landslide analysis. This dataset was generated through interferometric analysis and processing of Sentinel-1 radar imagery. Specifically, the Ortho dataset displays purely vertical displacements, visualized as a vector map of measurement points, each coloured according to average velocity. Each point on the map is associated with a time series of displacements, representing the displacement values for each satellite acquisition over time.

From the EGMS Ortho dataset, it is evident that the Pikote landslide has been moving very slowly from January 2019 to October 2023. However, considering the history of the landslide, particularly the significant event in 1997, the possibility of sudden mobilization of material due to scarp retreat cannot be excluded.

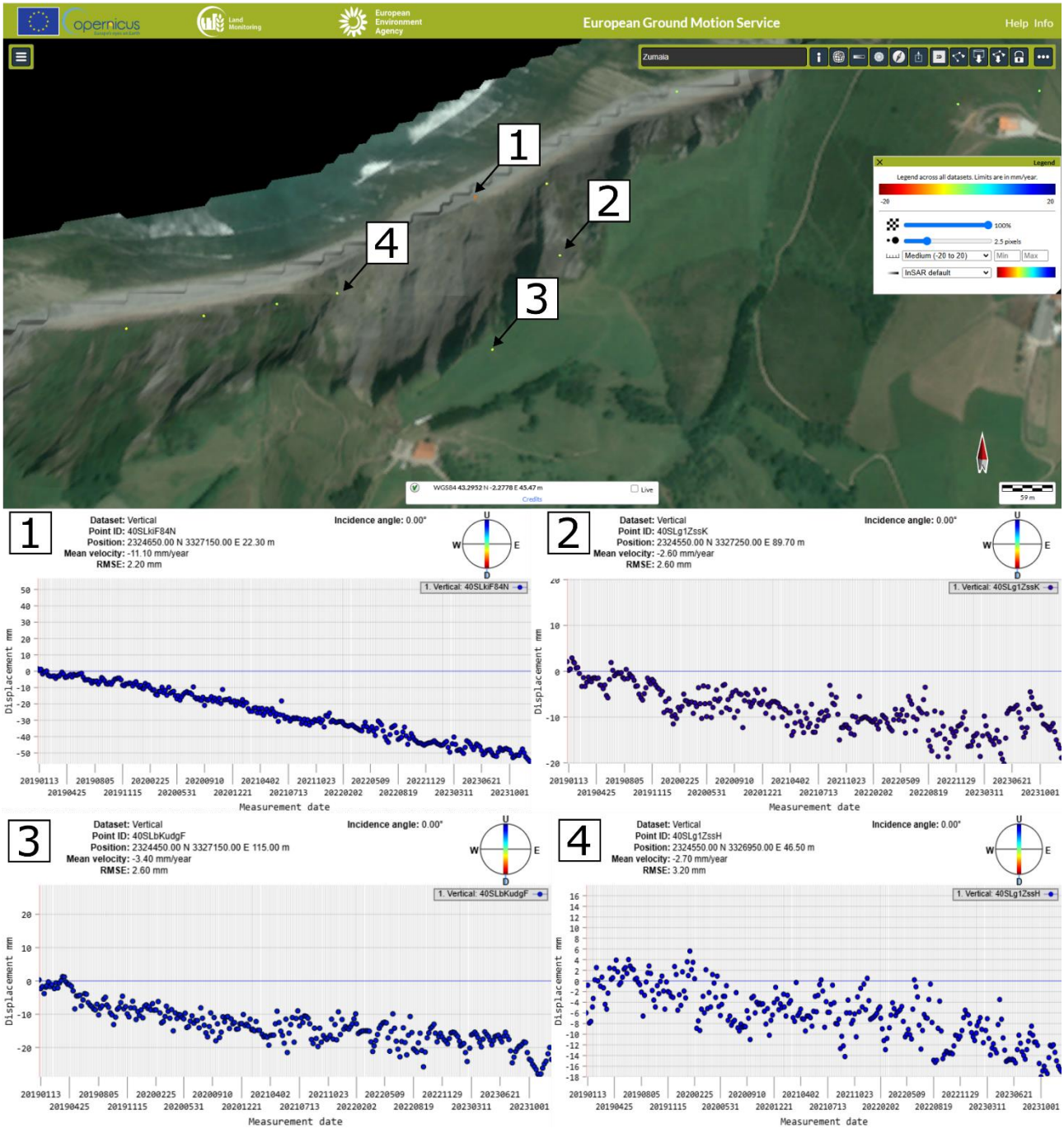

Fig. 39. EGMS Ortho dataset provides purely vertical displacements with a resolution of 100 m × 100 m. The dots indicate measurement points coloured by average vertical velocity. Each point is associated with a time series of displacement, i.e. a plot with values of displacement per each satellite acquisition.

Due to its complex mechanical behaviour and widespread and recurrent activity, the landslide deserves a tailored detailed investigation, in order to properly assess its current and future trend of activit,y which would be crucial in the context of hazard and risk assessment. In fact, beach visitors may be endangered by detachment of material reaching the shoreline whilst the building located above the landslide scarp may be affected by progressive head scarp retreat.

As illustrated in section 4.1, landslides occurring in flysch terrains can cause deformation and folding of the rock layers. The Pikote landslide is a notable example, as shown in Fig. 40.

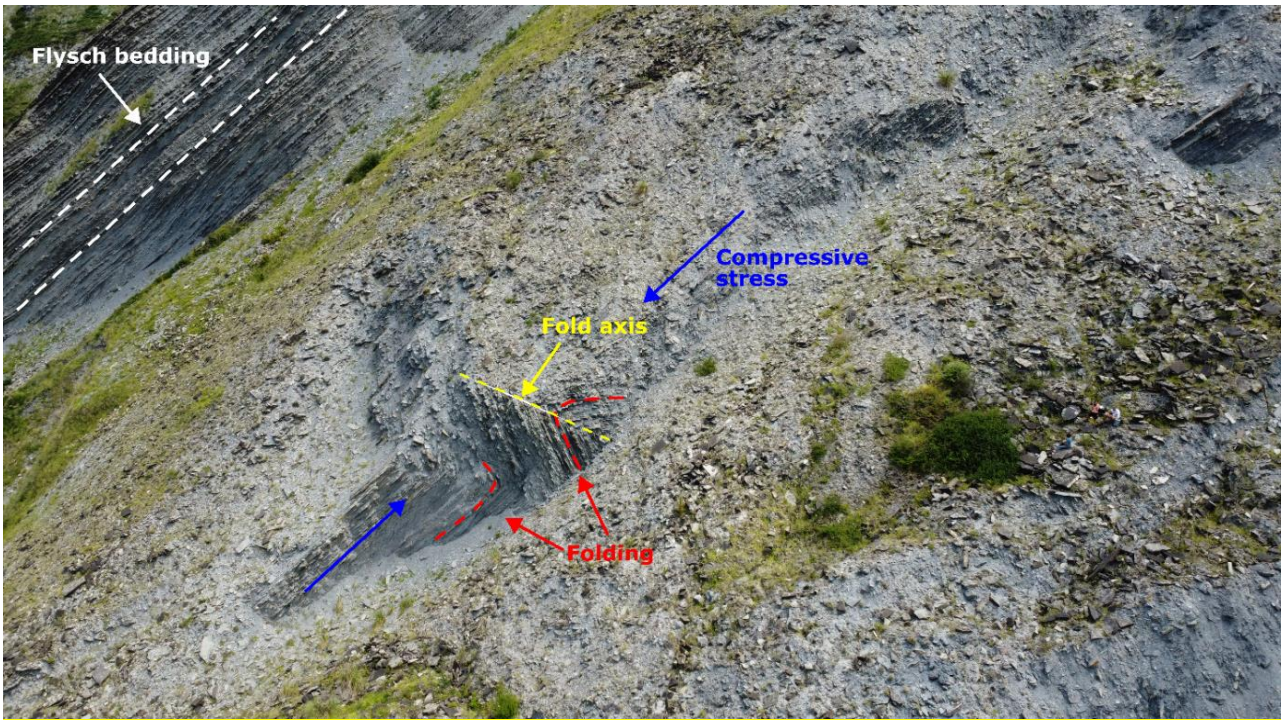

Fig. 40. Drone photograph captures a fold structure in flysch at Pikote landslide area, likely caused by the deformation due to downslope movement of the landslide body. The fold has as a metric extension and is located on the eastern flank of the landslide.

The fold shown on Fig. 40 may be described as a close fold with an interlimb angle around 60°, a structure formed under compressive forces. The fold axis is oriented nearly perpendicular to the bedding planes, highlighting lateral compressive stress. This folding likely emerged due to compressional stresses at the edges of a sliding rock wedge, constrained by underlying rock and overburden weight. The rock layers appear to have deformed slowly (creeping) under stress, adopting a visco-plastic rather than brittle behaviour. The primary stress direction, parallel to bedding and shear surfaces, facilitated folding along these planes.

This gradual, visco-plastic response suggests the rocks responded to sustained low-strain rates, which typically enhance ductility in otherwise brittle sedimentary layers. Creep deformation in these layers is also associated with specific conditions such as prolonged subsurface confinement and periodic loading, like seasonal variations in moisture content, which can further soften weaker layers and support slow plastic flow. This aligns well with landslide-induced deformations in flysch, where the combination of lateral compression and shear results in complex folding and bending patterns. As pointed out by Cruden and Varnes (1996), when the shear surface aligns with a discontinuity that runs parallel to the slope, the leading edge (or toe) of the displaced mass may create a wedge shape. This wedge can push into or override the stationary material in front of it, resulting in folding that extends beyond the initial rupture surface.

4.3. Baratzazarrak landslide

The landslide located at Baratzazarrak is accessible from a path descending from Elorriaga recreational area to the beach. Its length along the coastline is some 380 m, while the width varies from approximately 280 m in the central part to 130 m at its western flank (Fig. 41). The edge of the landslide scarp has an approximate length of 550 m and the landslide deposits cover an area of 60,000 m^2.

As for the Pikote landslide, the description below is based on varied sources of information: (a) field observations carried out along the landslide body and at its toe; (b) photographs, also taken with the drone, acquired during field surveys carried out in July 2024; (c) high-resolution DTM of the area; (d) multitemporal orthophoto images from 1945 to 2022; and (e) European Ground Motion Service (EGMS) dataset providing information on surficial movements.

The Baratzazarrak mass movement can be classified as a complex landslide. Field observations of landforms indicate a complex style of activity, including both a main rotational movement and secondary translational sliding testified by planar shear surfaces within the landslide body. Additionally, debris flows have been observed along the cliffs bordering the landslide flanks, highlighting active geomorphic processes on the slope.

Fig. 41. Panoramic view of the Baratzazarrak landslide taken by a drone. The lower part of the colluvium (in front of the path) is undercut by a low marine cliff, up to 10 m high.

Historical orthophotos dating back to 1945 provide further insights. These aerial photographs confirm that the Baratzazarrak landslide pre-dates 1945–46, as they show the landslide deposit already in place and covered by vegetation (Fig. 42). Since that time, the landslide has experienced periodic localized reactivations. In particular, orthophotos from 1977–78 and 2012 reveal fresh shear surfaces characterized by exposed, vegetation-free rock planes. Notably, the orthophotos from 1977–78 also indicate a potential debris flow along the eastern flank, further illustrating the highly dynamic nature of the slope.

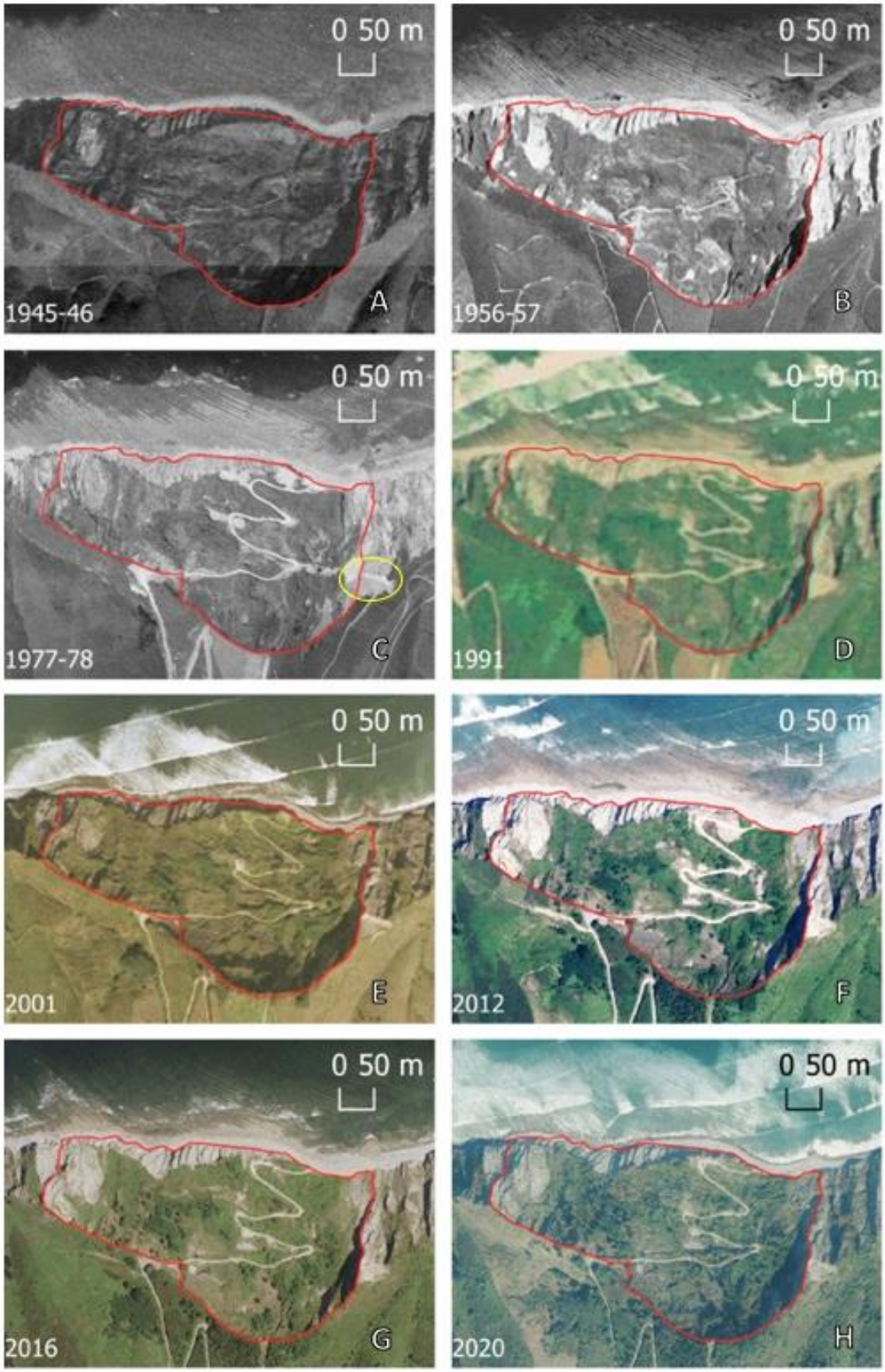

Fig. 42. Orthophoto images of Baratzazarrak landslide from 1945 to 2019. The red solid line indicates the approximate extension of the Baratzazarrak landslide area as it appears in the orthophoto of the year 2019. The yellow oval in (C) highlights the area where a debris flow occurred.

The comparison of Digital Terrain Models (DTMs) from 2017 and 2008, using the DEM of Difference (DoD) technique to calculate elevation changes, did not reveal substantial displacement across most of the landslide area (Fig. 43). Notable elevation changes were observed primarily along and near the path crosscutting the landslide, likely as a result of human activities and modifications in this area. However, it is important to note that the DTMs used have a spatial resolution of 1 m × 1 m, which limits the accuracy of the analysis. This resolution may not be adequate to detect smaller displacements with a high level of precision. Consequently, there is a need for additional, higher-resolution investigations — such as the use of more refined DTMs or ground-based monitoring — to more accurately capture and quantify smaller-scale displacements. Such data would enable a clearer understanding of both the mode and rate of landslide movement and allow for more accurate assessment of any ongoing instability within the landslide area.

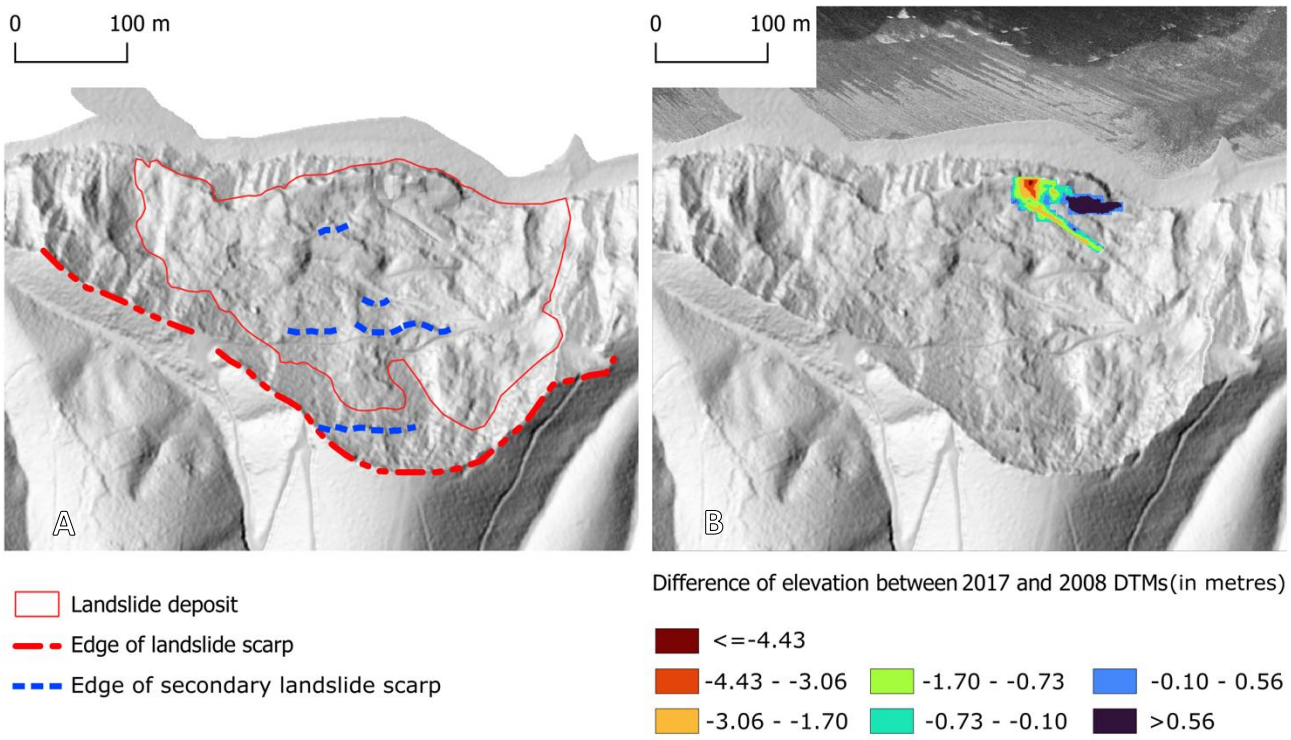

Fig. 43. (A) Baratzazarrak landslide on shaded relief obtained from a high-resolution DTM of 2017. The edges on the main scarp and seondary scarps are outlined. (B) DEM of Difference (DoD) for the years 2017–2008 showing that the changes in elevation mainly occurred along the path crossing the landslide body. Areas where no changes occurred are left non-coloured.

Fig. 44 presents the EGMS Calibrated dataset generated from interferometric analysis of Sentinel-1 radar images at full resolution (20 m × 5 m). The EGMS Calibrated data are displayed as a vector map of measurement points, colour-coded by average velocity. Each point is associated with a displacement time series, showing displacement values per satellite acquisition. Analysis of the EGMS dataset from 2019 to 2023 revealed few measurement points within the landslide deposit, while a considerable number are located in the distal area. The latter show mainly surface lowering at rates up to a maximum of 11.8 mm/year towards the west.

Slow displacement rate highlighted by interferometric data is compatible with visco-plastic deformations occurring at the landslide flanks which generate folding of the flysch strata as shown in Fig. 45. Structures of this kind occur in several places along the vertical profile of the landslide, at similar elevations, e.g. at +48 m and +61 m in respect to the cliff base as a reference level (Fig. 46). In fact, they are also common further to the west, all along the cliff towards Sakoneta, indicating widespread extent of downslope movement of flysch slabs, from 2–3 m to more than 10 m thick.

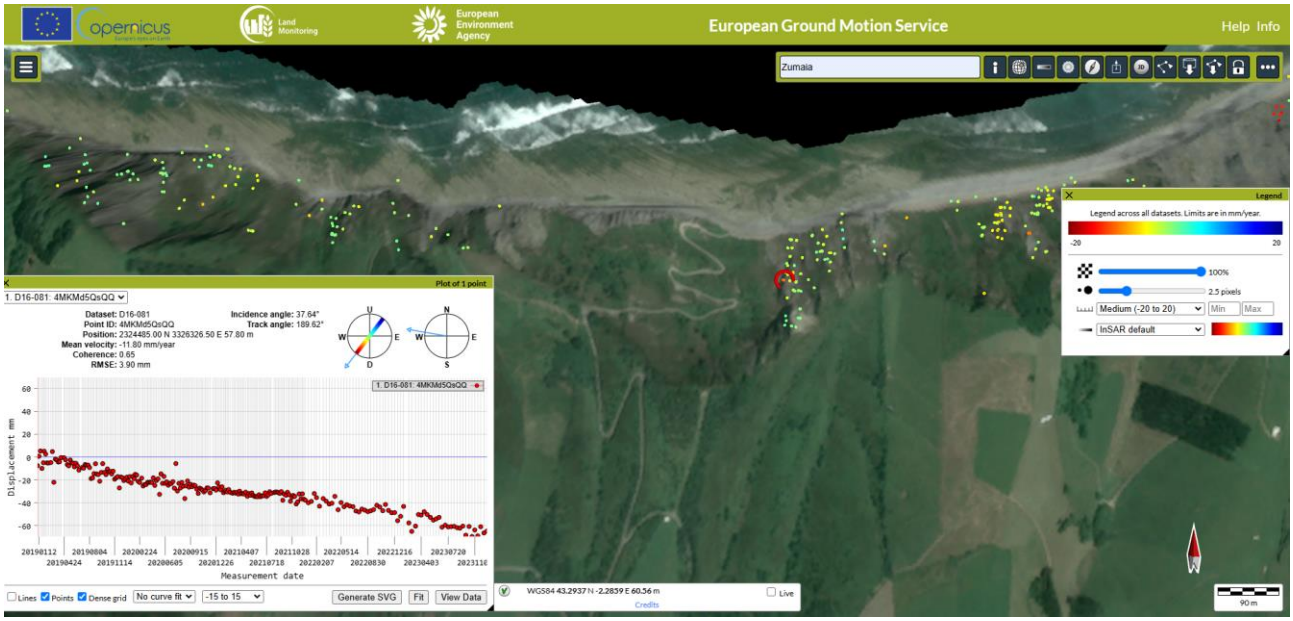

Fig. 44. EGMS Calibrated dataset the EGMS Calibrated dataset generated from interferometric analysis of Sentinel-1 radar images at full resolution (20 m × 5 m). Dots indicate measurement points coloured by average vertical velocity. Each point is associated with a time series of displacement, i.e. a plot with values of displacement per each satellite acquisition.

The evidence of deformation of flysch beds was also observed at the level of wave-cut platform immediately in front of an eroded toe of the landslide (Fig. 47). Normally, flysch layers follow WNW–ESE strike and dip towards the north at an angle of 20–30° (see Fig. 20, 22B), but in the platform section adjacent to the Baratzazarrak landslide the arrangement of strata is different. In plan, they follow a semi-circular pattern, pointing towards the sea, whereas in cross-section their dip is much steeper, locally up to vertical and even overturned (i.e., dipping to the south). These anomalously dipping strata hide under the landslide colluvium. In addition, the strata are heavily broken along densely spaced fractures. Remarkable is the sharp boundary between the deformed and undeformed flysch (Fig. 47). The presence of deformed flysch beds is tentatively interpreted as resulting from a heavy load imposed by the displaced landslide masses, although the colluvium (and perhaps part of flysch bedrock as well) has already been eroded by waves, exposing bedrock previously concealed beneath it.

Fig. 45. Visco-plastic deformation in flysch in the Baratzazarrak landslide deposit.

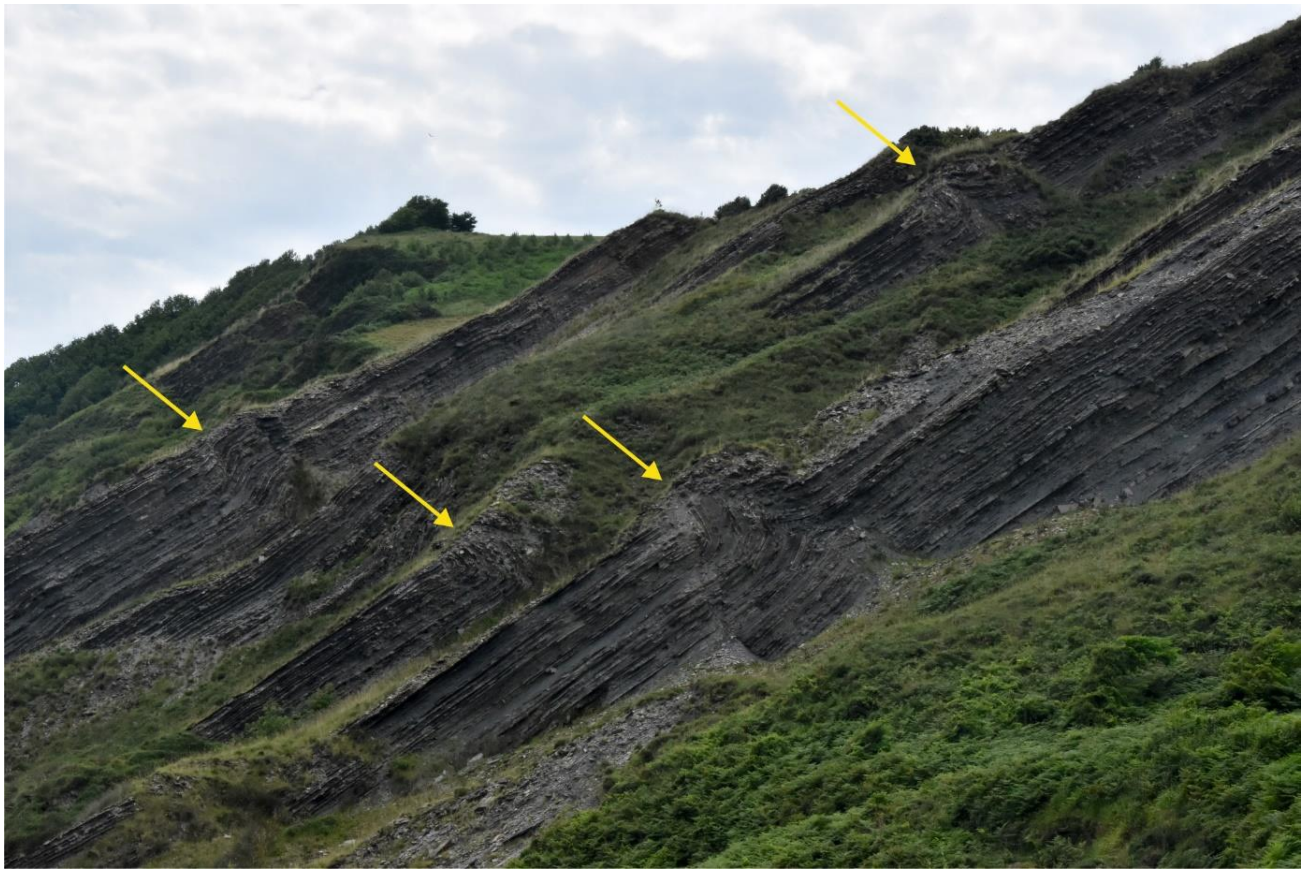

Fig. 46. Multiple deformations of flysch beds exposed in the lateral sides of displaced landslide blocks (highlighted by arrows).

Fig. 47. Landslide-induced deformation of flysch beds exposed in the level of the wave-cut platform. Note sharp contact (yellow broken line) between deformed and undeformed flysch. People provide the scale.

4.4. Mendatagaina landslide complex

The landslide complex situated to the west of Mendatagaina promontory is probably the largest one developed in the "black flysch". Its length along the coastline is more than 1.2 km, whereas the width varies from approximately 100 m in the westernmost part to 500 m in the eastern part. Exploration of the landslide-affected area was difficult because of extremely dense vegetation over most of its area. Therefore, the description below is based on four sources of information: (a) high-resolution DTM of the area; (b) a series of images from Google Earth, covering the last 20 years; (c) general view from the viewing point on Mendatagaina promontory; (d) observations from a red-marked trail that uses the former railway track crossing the landslide area. It is preliminary and partly tentative, and should be supported by more detailed analysis and systematic field inspection.

Inspection of the DTM (Fig. 48) shows that the landslide area is morphologically very complex and likely consists of several individual landslide bodies, which may have been active at different times. In addition, subsequent displacements have occurred within larger landslides and the area seems to be active until now. The model suggests the existence of at least three separate units. Unit (A) is a complex landslide which has developed retrogressively most inland and is currently approximately 500 m long. The most elevated part of the landslide crown is at 150 m a.s.l. The upper part of the landslide represents irregular hummocky terrain, now largely overgrown by forest (Fig. 49), whereas the lower part seems to consist of more coherent blocks. Fig. 50 shows the ground view of unit (A), as seen from the viewing point on the promontory. Comparison of satellite images for the part close to the coastline shows the evolution of secondary head scarps and slides (Fig. 51).

The landslide unit (B) did not advance inland as much as unit (A) and probably consists of several displaced blocks, whose internal deformation during movement gave rise to the rough, heavily vegetated terrain (Fig. 48). It is approximately 450 m long and up to 250 m wide, with elevation difference of 120 m. Minor secondary slides affect the frontal part, possibly triggered by wave undercutting of colluvial complexes (Fig. 52).

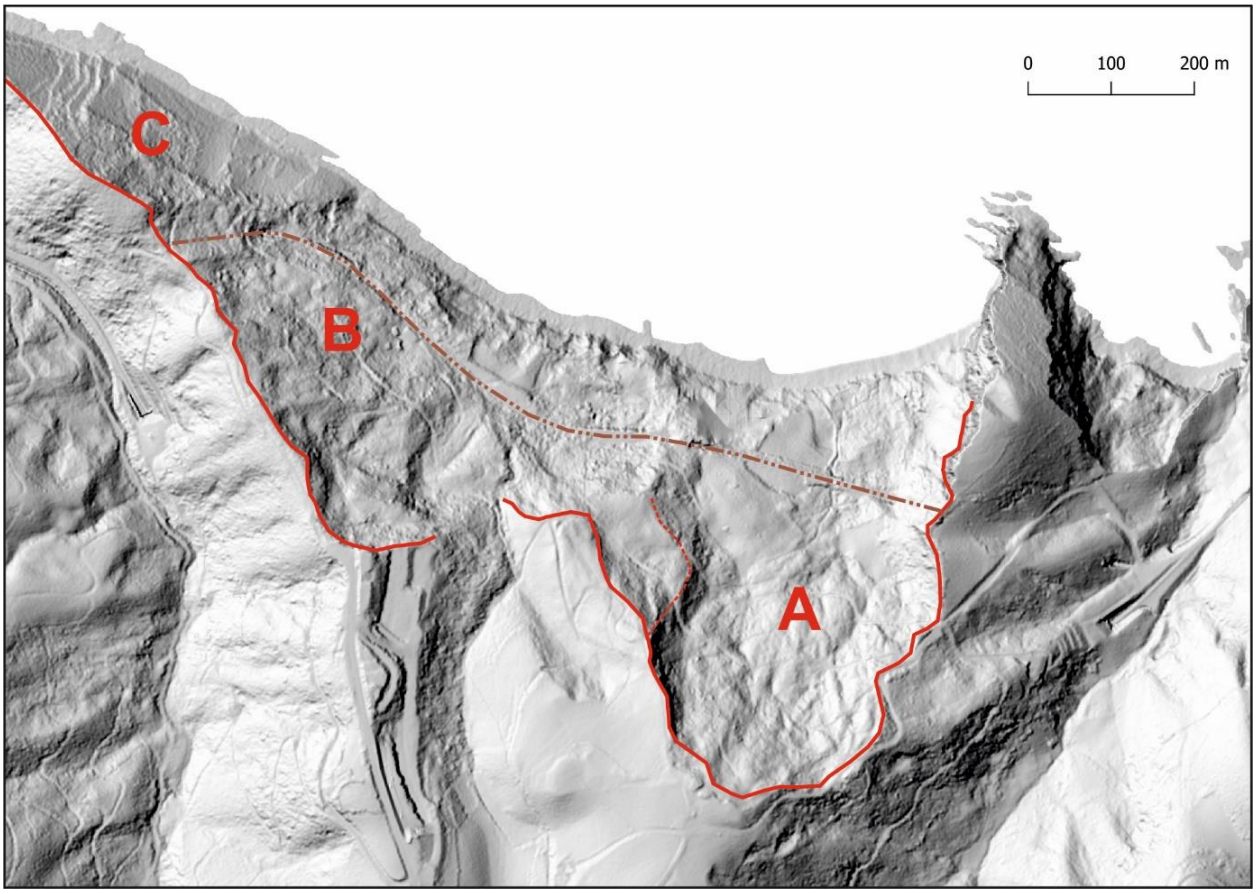

Fig. 48. Landslide area to the west of Mendatagaina promontory on high-resolution DTM. Solid red line indicates an approximate course of the landslide crown, broken brown line shows the course of an abandoned railway track.

Fig. 49. The eastern part of the landslide area is now largely overgrown by forest.

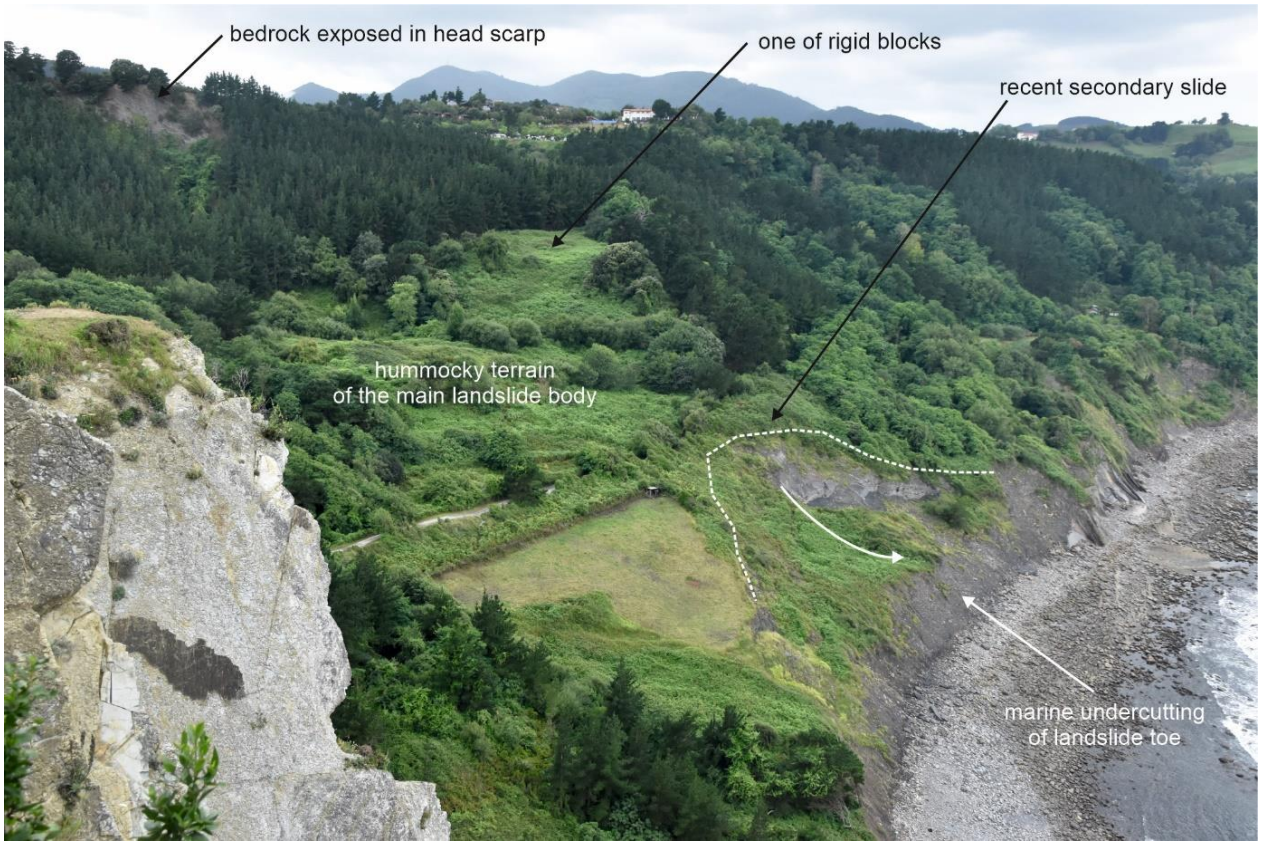

Fig. 50. Annotated photograph of landslide unit (A).

Further to the west extends the landslide unit (C), which represents a complex translational slide. Coast-parallel bedding surfaces, inclined to the north, acted as slip planes (Fig. 53). It is very likely that different sections of this unit moved at different times, and there were subsequent localized displacements within previously active sections. This is shown on Fig. 54, where two satellite images, from 2020 and 2024, are compared. They show that between 2020 and 2024 a small scar, originally some 18 m wide × 10 m long, expanded upslope and is now 28 m wide at the base and 26 m long. One can also see another displaced slab, which still carries the soil cover, along with a few trees, although these are not tilted. The volume of debris at the base of exposed slip planes appears small, which would testify to efficient removal of broken rock by waves, perhaps mainly during winter storms.

The landslide complex to the west of Mendatagaina deserves interest not only because it is large and complex, but also because the ongoing displacements within this area strongly interfered with human activity. The railway from Zumaia to Deba, opened in 1900, used to cross the landslide terrain between two tunnels, dug below the Mendatagaina promontory in the east and the Arranomendi hill in the west (Fig. 55). Apparently, ground instability caused persistent engineering problems and finally a decision was made to excavate another tunnel, further inland, and relocate the entire section away from the landslide terrain. The new tunnel was opened in 1988 and the old track abandoned and then converted into a hiking trail. Old tunnels are inaccessible, but a short tunnel in the middle of the abandoned stretch, approximately 50 m long, is now used by the trail (Fig. 56A). Although the track itself was dismantled, one can still see ground surface deformations along the embankment, including wavy sections, effects of downslope sliding, as well as transverse steps up to several metres in height in total (Fig. 56B). The coexistence of the complex landslide and the abandoned railway track opens various interpretation opportunities, focused on nature-human interactions, natural hazards, and the necessity of proper landform recognition prior to undertaking major engineering works.

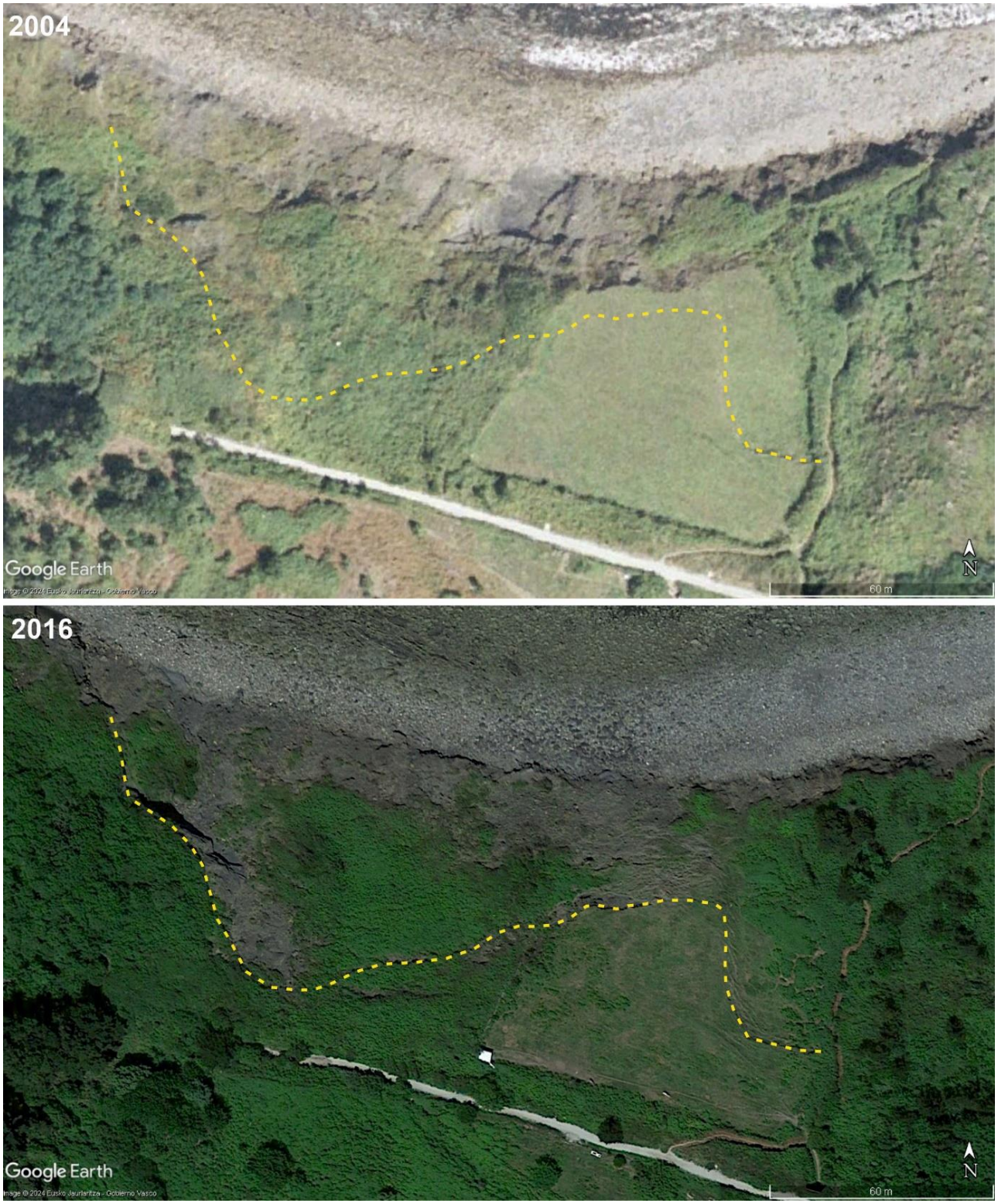

Fig. 51. The seaward part of landslide unit (A) on Google Earth imagery from 2004 and 2016. Dashed yellow line shows the position of landslide crown in 2016 and is superimposed on the older photo for comparison. Compare also with Fig. 50, where this landslide is labelled as “recent secondary slide”.

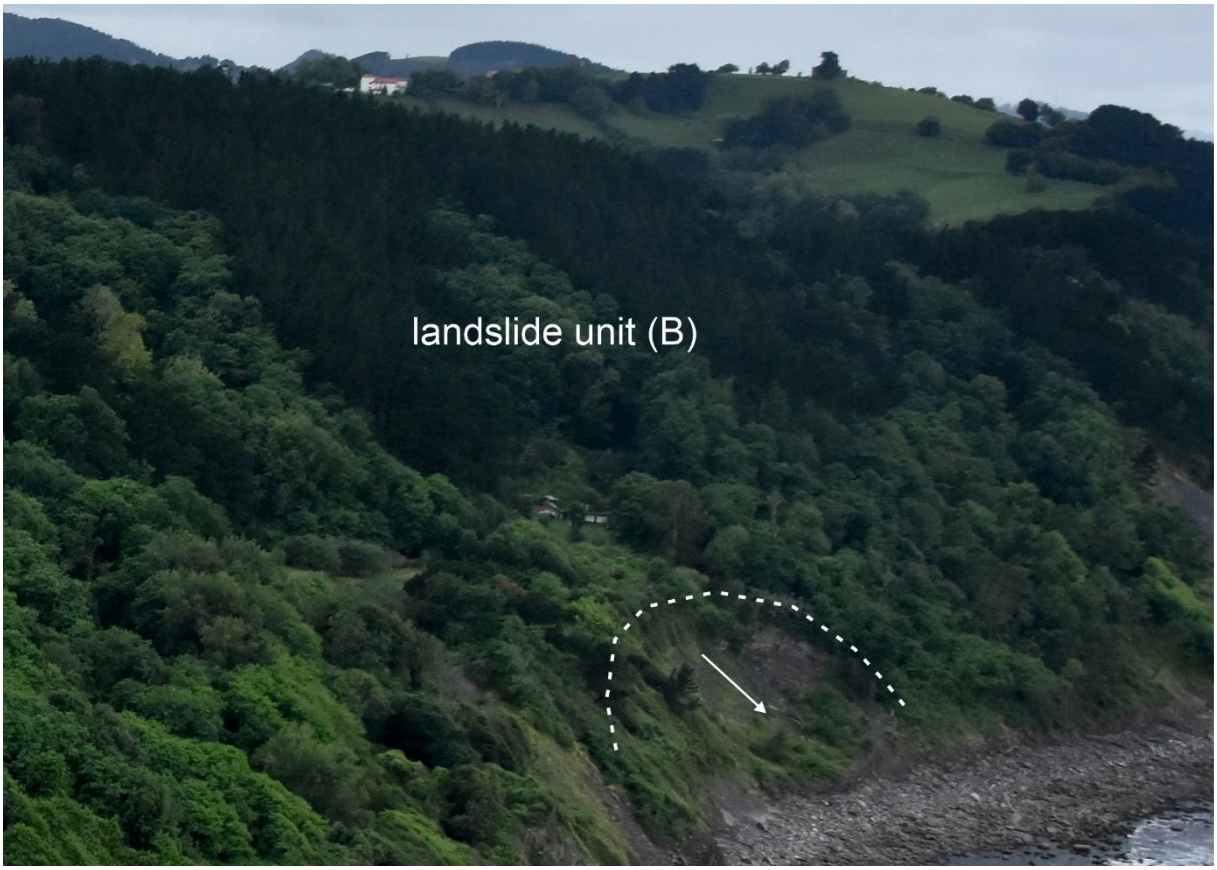

Fig. 52. Details of morphology of landslide unit (B) are completely hidden by vegetation, but the presence of secondary slides in the toe part can be clearly seen from the viewing point on Mendatagaina promontory.

Fig. 53. Landslide unit (C) with exposed slip planes, fresh debris consisting of broken slabs of shale at the transition to the wave-cut platform, and tilted trees on the most recently displaced part.

Fig. 54. Westernmost part of Mendatagaina landslide complex, with evidence of minor slides within previously exposed rock slabs (inside the yellow rectangle).

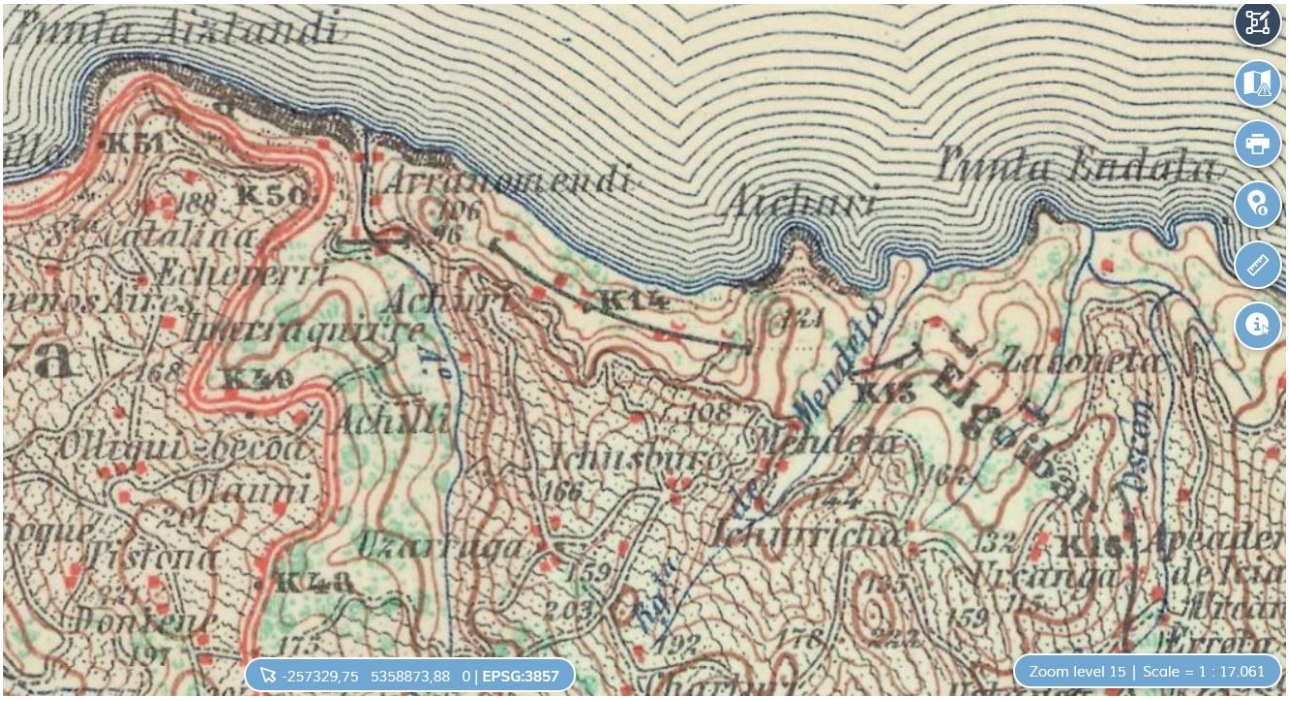

Fig. 55. An old map showing the original course of the railway track across the landslide – section labelled as K14 (source: https://www.ign.es/iberpix/visor/).

Fig. 56. Abandoned section of the railway across the landslide terrain, now a hiking trail. A – old tunnel, B – ground displacements along the embankment.

5. Conclusions and outlook

This report summarizes results of Phase 1 of the project intended to facilitate better understanding of coastal landforms in the Basque Coast UNESCO Global Geopark, with particular focus on landslides. The key achievements include:

- elaboration of an inventory of landforms present in the coastal stretch between Zumaia and Ondarroa, divided into two fundamental units: cliffs and wave-cut platforms.
- photographic documentation of the rich landform inventory, which can be used for various education and interpretation activities in the Geopark.
- recognition of two major landslide complexes present in the calcareous flysch between Zumaia and Sakoneta, representing two different states of activity.
- recognition of landslide-induced deformations of flysch strata, involving bending and compressional folding.
- evaluation of displacement history of these landslides from the mid-20th century, using different sources of information.
- reconnaissance mapping of a large landslide complex in "black flysch", to the west of Mendatagaina.

The work executed in Phase 1 sets the possible goals for the follow-up of the project, planned for 2025. On the one hand, it will be focused on more detailed mapping and analysis of Pikote and Baratzazarrak landslides, including deformation structures recognized at the level of the wave-cut platform and landslide deposits exposed in the low cliffs cut in the colluvium. On the other hand, the landform inventory will be the basis for a geomorphological map of the coastal zone of the Basque Coast UNESCO Global Geopark.

Further options include more detailed research on morphology of coastal platforms in "black flysch", which are clearly different from the better-known platforms in the calcareous flysch, more systematic research focused on quantification of relief diversity of wave-cut platforms in the calcareous flysch, and more detailed mapping and analysis of other landslides in the coastal belt.

References

Aranburu, A., Arriolabengoa, M., Iriarte, E., Giralt, S., Yusta, I., Martínez-Pillado, V., Del Val, M., Moreno, J., Jiménez-Sánchez, M., 2015. Karst landscape evolution in the littoral area of the Bay of Biscay (north Iberian Peninsula). Quaternary International 364, 217–230. https://doi.org/10.1016/j.quaint.2014.09.025

Cearreta, A., Irabien, M.J., Gómez Arozamena, J.E., El Bani Altuna, N., Goffard, A., García-Artola, A., 2021. Environmental evolution of the Basque Coast Geopark estuaries (southern Bay of Biscay) during the last 10,000 years. Journal of Marine Systems 219, 103557. https://doi.org/10.1016/j.jmarsys.2021.103557

Cruden, D.M., Varnes, D.J., 1996. Landslide types and processes. In: Turner, A.K., Schuster, R.L. (Eds.), Landslides: Investigation and Mitigation. Transportation Research Board Special Report 247, pp. 36–75.

Hilario, A., Mendia, M., Agirrezabala, L.M., Aramburu, A., Arriolabengoa, M., Orue-Etxebarria, X., Monge-Ganuzas, M., Mugerza, I., García, C., 2023. Lugares de interés geológico. 229 pp (accessible online at https://geoparkea.eus/site_media/pdf/INVENTARIO_LIG_Geoparkea.pdf)

Morales, T., Clemente, J.A., Damas Mollá, L., Izagirre, E., Uriarte, J.A., 2021. Analysis of instabilities in the Basque Coast Geopark coastal cliffs for its environmentally friendly management (Basque-Cantabrian basin, northern Spain). Engineering Geology 283, 106023. https://doi.org/10.1016/j.enggeo.2021.106023